J|A|C|S
ARTICLES
Published on Web 01/17/2006

Ruthenium Molecular Wires with Conjugated Bridging Ligands: Onset of Band Formation in Linear Inorganic Conjugated Oligomers

Samuel Flores-Torres,[†] Geoffrey R. Hutchison,[†] Leonard J. Soltzberg,[‡] and Héctor D. Abruña*,[†]

Contribution from the Department of Chemistry and Chemical Biology, Baker Laboratory, Cornell University, Ithaca, New York 14853-1301, and Department of Chemistry, Simmons College, 300 The Fenway, Boston, Massachusetts 02115

Received August 1, 2005; E-mail: hda1@cornell.edu

Abstract: We have prepared and characterized a series of multimetallic oligomers of Ru using the π-conjugated bridging ligand tetra-2-pyridyl-1,4-pyrazine (tppz), as well as mixed-ligand complexes with terpyridine end caps, and analyzed their electrochemical and spectroscopic properties, comparing them with modern computational electronic structure methods. The results suggest that the high degree of metal−metal interunit communication in these linear oligomers yields low HOMO−LUMO gaps, high delocalization, and the onset of "quasi-band" features, all indicative that these compounds should be excellent molecular wire materials. Recent spectroscopic and excited-state analyses of these and related compounds focus on optically accessible states, which ignore optically silent frontier electronic states more relevant to nanoelectronic applications.

Introduction

One-dimensional oligomeric and polymeric conjugated materials with a high degree of electronic communication along the chain have long been studied in the form of transition-metal complexes and more recently in the form of organic conjugated materials such as polyacetylene, polythiophene, polypyrrole, polyaniline, and others.[1] These materials have gained renewed interest in the form of applications as potential "molecular wire" compounds for nanometer-scale electronic devices as well as improving fundamental scientific understanding of electronic materials from a "bottom-up" approach. Many techniques exist to probe charge-transfer mechanisms and rates through such linear molecules, including single-molecule electronic measurements,[2−5] as well as more conventional electrochemical and spectroelectrochemical methods.[2,5−11] Furthermore, chemical modification to illustrate structural relationships will be needed to solve challenges such as molecular stability, molecular-metal contact stability, and the onset of band formation from quantized molecular electronic structure.

Transition-metal complexes incorporating π-conjugated bridging ligands are extremely attractive as potential linear molecular wires because of high stability, the accessibility of multiple stable redox states, and the ability to synthetically tailor both the ligand itself as well as utilizing a wide range of metal ions to form complexes. Bimetallic and trimetallic complexes, particularly those of cobalt, ruthenium, and osmium, have previously been studied via electrochemistry.[2,7,11−38] In the limit

[†] Cornell University.
[‡] Simmons College.

(1) MacDiarmid, A. G. *Synth. Met.* **2001**, *125*, 11.
(2) Tsuda, A.; Osuka, A. *Science* **2001**, *293*, 79.
(3) McCreery, R. L. *Chem. Mater.* **2004**, *16*, 4477.
(4) Liang, W. J.; Shores, M. P.; Bockrath, M.; Long, J. R.; Park, H. *Nature* **2002**, *417*, 725.
(5) Park, J.; Pasupathy, A. N.; Goldsmith, J. I.; Chang, C.; Yaish, Y.; Petta, J. R.; Rinkoski, M.; Sethna, J. P.; Abruña, H. D.; McEuen, P. L.; Ralph, D. C. *Nature* **2002**, *417*, 722.
(6) Molnar, S. M.; Jensen, G. E.; Brewer, K. J. *Abstr. Pap. Am. Chem. Soc.* **1994**, *207*, 219.
(7) Demadis, K. D.; Hartshorn, C. M.; Meyer, T. J. *Chem. Rev.* **2001**, *101*, 2655.
(8) Robin, M. B.; Day, P. *Advances in Inorganic Chemistry and Radiochemistry*; Academic Press: New York, 1967; Vol. 10.
(9) Park, J. W.; Pasupathy, A. N.; Goldsmith, J. I.; Soldatov, A. V.; Chang, C.; Yaish, Y.; Sethna, J. P.; Abruña, H. D.; Ralph, D. C.; McEuen, P. L. *Thin Solid Films* **2003**, *438*, 457.
(10) Dattelbaum, D. M.; Hartshorn, C. M.; Meyer, T. J. *J. Am. Chem. Soc.* **2002**, *124*, 4938.
(11) Powers, M. J.; Meyer, T. J. *Inorg. Chem.* **1978**, *17*, 1785.
(12) Wacholtz, W. F.; Fischer, S. H.; Schmehl, R. H.; Auerbach, R. A. *Abstr. Pap. Am. Chem. Soc.* **1987**, *194*, 424.
(13) Ward, M. D.; McCleverty, J. A. *J. Chem. Soc., Dalton Trans.* **2002**, 275.
(14) DelNegro, A. S.; Woessner, S. M.; Sullivan, B. P.; Dattelbaum, D. M.; Schoonover, J. R. *Inorg. Chem.* **2001**, *40*, 5056.
(15) Brennan, J. L.; Howlett, M.; Forster, R. J. *Faraday Discuss.* **2002**, *121*, 391.
(16) Chanda, N.; Sarkar, B.; Kar, S.; Fiedler, J.; Kaim, W.; Lahiri, G. K. *Inorg. Chem.* **2004**, *43*, 5128.
(17) Denti, G.; Campagna, S.; Sabatino, L.; Serrni, S.; Ciano, M.; Balzani, V. *Inorg. Chem.* **1990**, *29*, 4750.
(18) Marcaccio, M.; Paolucci, F.; Paradisi, C.; Carano, M.; Roffia, S.; Fontanesi, C.; Yellowlees, L. J.; Serroni, S.; Campagna, S.; Balzani, V. *J Electroanal. Chem.* **2002**, *532*, 99.
(19) Martin, R. E.; Diederich, F. *Angew. Chem., Int. Ed. Engl.* **1999**, *38*, 1350.
(20) Powers, M. J.; Callahan, R. W.; Salmon, D. J.; Meyer, T. J. *Inorg. Chem.* **1976**, *15*, 894.
(21) Flanagan, J. B.; Margel, S.; Bard, A. J.; Anson, F. C. *J. Am. Chem. Soc.* **1978**, *100*, 4248.
(22) Johnson, E. C.; Sullivan, B. P.; Salmon, D. J.; Adeyemi, S. A.; Meyer, T. J. *Inorg. Chem.* **1978**, *17*, 2211.
(23) Powers, M. J.; Meyer, T. J. *Inorg. Chem.* **1978**, *17*, 2955.
(24) Sullivan, B. P.; Meyer, T. J. *Inorg. Chem.* **1980**, *19*, 752.
(25) Demadis, K. D.; Neyhart, G. A.; Kober, E. M.; White, P. S.; Meyer, T. J. *Inorg. Chem.* **1999**, *38*, 5948.
(26) Belser, P.; Bernhard, S.; Jandrasics, E.; von Zelewsky, A.; DeCola, L.; Balzani, V. *Coord. Chem. Rev.* **1997**, *159*, 1.

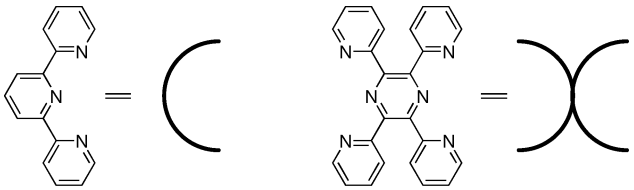

Figure 1. Tridentate π-conjugated ligands terpyridine (tpy) and tetra-2-pyridyl-1,4-pyrazine (tppz).

of zero communication between metal centers, only one oxidation peak will be observed (as a two-electron process), so if multiple oxidation peaks are observed, the separation between the peaks indicates the degree of communication—although the increase in electronic repulsion, as well as statistical factors, needs to be taken into account.[21] Tridentate bridging ligands, such as tetra-2-pyridyl-1,4-pyrazine (tppz) (Figure 1), are particularly attractive since a linear one-dimensional geometry is enforced when bound to octahedral transition-metal ions.

Our group has previously studied monomeric, dimeric, and oligomeric tppz/tpy transition-metal complexes in isolation,[39] as well as in two or three-dimensional ordered arrays of tppz chain complexes.[26,30,40−42] Recently, ruthenium tppz oligomers and polymers were studied via spectroscopy and time-dependent density functional theory (TDDFT).[43] However, this study did not yield significant information on the ground-state electronic structure via electrochemistry or computational methods. Since optical absorption reveals only symmetry-allowed transitions, while electrochemistry or single-molecule electronic measurements can access the entire molecular electronic structure, the fundamental study of the longer multimetallic oligomers remains to be addressed and should yield insight into the distance dependence of charge transfer and the nature of electronic communication between metal centers in delocalized chains.

In this contribution, we report the synthesis, characterization via electrochemistry, spectroscopy, MALDI-TOF mass spectrometry, and computational modeling of two series of ruthenium oligomers with the tppz π-bridging ligand as indicated in Figure 2. The use of both terpyridine and tppz-capped oligomers demonstrates the sensitivity of the complexes to ligand substitution. This full analysis of the electronic structure of these compounds demonstrates the high degree of electronic coupling and tremendous potential for highly conductive one-dimensional molecular wires in transition-metal oligomers.

Experimental Section

Materials and Instrumentation. All solvents and reagents for synthesis were purchased from Aldrich as at least reagent grade quality and used without further purification. Acetonitrile, used for electrochemical and spectroscopic experiments, was purchased from Burdick and Jackson and was dried over 4-Å molecular sieves for at least 48 h before use. The supporting electrolyte for electrochemical measurements, tetra-*n*-butylammonium hexafluorophosphate (TBAH) (GFS Chemicals), was recrystallized three times from ethyl acetate and dried under vacuum for 96 h and used at 0.1 M concentration.

All cyclic voltammetry (CV) and differential pulse voltammetry (DPV) measurements were taken using a CV-27 (BAS) or an Epsilon (BAS) potentiostat, and data were directly recorded with custom data collection software. The reference electrode used was Ag/AgCl with a large-area coiled Pt wire counter electrode.

Optical ultraviolet−visible (UV/vis) absorption spectra were obtained using a HP 8453 diode array spectrometer at room temperature in acetonitrile, unless otherwise stated with conventional 1.0 cm quartz cells. All optical ultraviolet−visible−near-infrared (UV/vis/NIR) spectra were obtained using a double-beam Shimadzu UV-3101PC UV/vis/near-IR Spectrophotometer with quartz cells and dry acetonitrile. MALDI-TOF positive ion data were obtained with a Bruker Omniflex run in linear mode and a Waters Micromass MALDI micro MX run in reflectron mode.

Synthesis of Ruthenium Oligomers and Polymers. The syntheses of the monomers and dimers of both series **1** and **2** and series **3** were published previously[39] and were performed here without further modification.

[Ru$_n$(tppz)$_{n+1}$] Polymer. A stepwise building block approach was utilized to synthesize the polymers by allowing separation of high molecular weight species, which are otherwise very difficult to purify when synthesized via performing uncontrolled polymerizations. To a solution of Ru(tppz)$_2$(PF$_6$)$_2$ or Ru$_2$(tppz)$_3$(PF$_6$)$_4$ (25 μmol) in ethylene glycol (20 mL) was added Ru(tppz)Cl$_3$ or Ru(tpy)Cl$_3$ (0.1 mmol). The solvent was purged with nitrogen (before adding the chemical or heating) and heated for 12 h or placed in a microwave for a total of 8−12 min (in six 2-min intervals). The resulting blue solution was cooled and filtered. The product was then precipitated with aqueous ammonium hexafluorophosphate, filtered out, washed with water, and dried by washing with diethyl ether. The resulting dark blue powder was purified via repeated column chromatography on neutral alumina with acetonitrile/toluene (1:1) as eluent in a gradient of methanol to move highly charged molecules. Since higher charged molecules elute more slowly, the first band is the monomer with an orange color and the second band includes the dimer with a violet color. The higher molecular weight oligomers are blue. (Common impurities include molecules missing one tppz ligand.) After elution of all monomer and dimer species, a gradient of methanol was used to elute any remaining highly charged molecules. All species were recrystallized in an acetonitrile/ether mixture by diffusion recrystallization.

Computational Methods. The geometry of both tpy-capped and tppz-capped oligomers of [Ru$_n$(tppz)$_{n+1}$]$^{2n+}$ and [(tpy)$_2$Ru$_n$(tppz)$_{n-1}$]$^{2n+}$ for lengths from 1 to 6 metal centers (i.e., $n = 1-6$) were computed via the UFF molecular mechanics method[44] and Gaussian 03.[45] The lowest-energy conformation of the oligomers was found to be a helical structure, as illustrated in Figure S5.

(27) Vogler, L. M.; Brewer, K. J. *Inorg. Chem.* **1996**, *35*, 818.
(28) Ishow, E.; Gourdon, A.; Launay, J. P.; Chiorboli, C.; Scandola, F. *Inorg. Chem.* **1999**, *38*, 1504.
(29) Demadis, K. D.; Neyhart, G. A.; Kober, E. M.; White, P. S.; Meyer, T. J. *Inorg. Chem.* **2000**, *39*, 3430.
(30) Bernhard, S.; Takada, K.; Diaz, D. J.; Abruña, H. D.; Murner, H. *J. Am. Chem. Soc.* **2001**, *123*, 10265.
(31) Del Guerzo, A.; Leroy, S.; Fages, F.; Schmehl, R. H. *Inorg. Chem.* **2002**, *41*, 359.
(32) Kober, E. M.; Caspar, J. V.; Sullivan, B. P.; Meyer, T. J. *Inorg. Chem.* **1988**, *27*, 4587.
(33) Kober, E. M.; Marshall, J. L.; Dressick, W. J.; Sullivan, B. P.; Caspar, J. V.; Meyer, T. J. *Inorg. Chem.* **1985**, *24*, 2755.
(34) Dodsworth, E. S.; Lever, A. B. P. *Chem. Phys. Lett.* **1986**, *124*, 152.
(35) Lever, A. B. P. *Inorg. Chem.* **1990**, *29*, 1271.
(36) Vlcek, A. A.; Dodsworth, E. S.; Pietro, W. J.; Lever, A. B. P. *Inorg. Chem.* **1995**, *34*, 1906.
(37) Luo, Y.; Potvin, P. G.; Tse, Y. H.; Lever, A. B. P. *Inorg. Chem.* **1996**, *35*, 5445.
(38) Gorelsky, S. I.; Lever, A. B. P. *J. Organomet. Chem.* **2001**, *635*, 187.
(39) Arana, C. R.; Abruña, H. D. *Inorg. Chem.* **1993**, *32*, 194.
(40) Blasini, D. R.; Flores-Torres, S.; Smilgies, D.-M.; Abruña, H. D. *Langmuir*, in press.
(41) Diaz, D. J.; Bernhard, S.; Storrier, G. D.; Abruña, H. D. **2001**, *105*, 8746.
(42) Diaz, D. J.; Storrier, G. D.; Bernhard, S.; Takada, K.; Abruña, H. D. **1999**, *15*, 7351.
(43) Fantacci, S.; De Angelis, F.; Wang, J. J.; Bernhard, S.; Selloni, A. *J. Am. Chem. Soc.* **2004**, *126*, 9715.
(44) Rappe, A. K.; Casewit, C. J.; Colwell, K. S.; Goddard, W. A.; Skiff, W. M. *J. Am. Chem. Soc.* **1992**, *114*, 10024.
(45) Frisch, M. J.; et al. *Gaussian 03*, revision B.04; Gaussian, Inc.: Wallingford, CT, 2004.

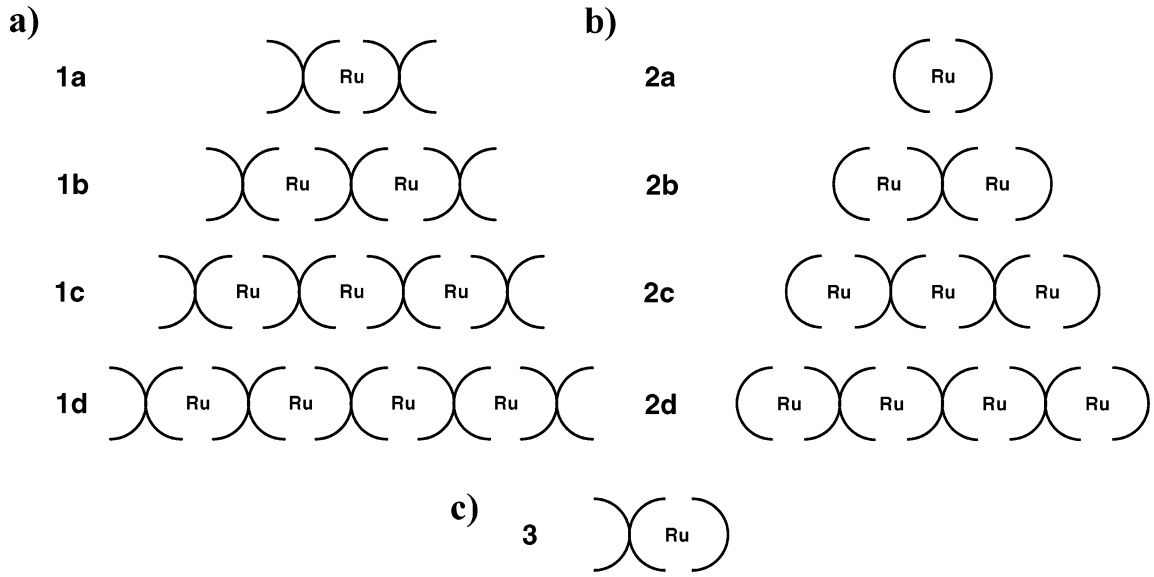

Figure 2. Scheme of ruthenium oligomers with tppz bridging ligands and (a) tppz end caps (series **1**) or (b) tpy end caps (series **2**) and (c) series **3**.

Electronic structures of the complexes were computed by single-point calculations using density functional theory (DFT) and the hybrid B3LYP functional[46,47] using the Lanl2DZ basis set[48−51] with relativistic effective core potentials,[49−51] which has been shown to yield reasonable accuracy for predictions of ionization potentials,[52] electron affinities,[52−57] HOMO−LUMO gaps,[58,59] and thus high correlations with electrochemical redox measurements. Additionally, the INDO semiempirical method was used to compute both ground-state electronic structure and INDO/S[60] excitation energies, using Ru and Fe parameters reported previously[61,62] via the CNDO program[63] and the standard active space of 10 occupied and 10 unoccupied orbitals. In similar mononuclear ruthenium diimine complexes, the INDO-computed electronic structure and INDO/S-computed excitation energies proved to be comparable in accuracy to DFT and TDDFT methods, respectively.[38]

Solvation of charged species, such as the transition-metal complexes studied here, involves screening by the surrounding dielectric, which has significant effects on the electronic structure and optical excitation energies. Therefore, in addition to the previously mentioned gas-phase calculations, the polarizable continuum model (PCM) solvation methodology[64−67] was used for computing ground-state B3LYP/Lanl2DZ electronic structures in acetonitrile using Gaussian03, as described below. Also, since the UFF molecular mechanics method does not account for delocalization across the entire oligomer or Jahn−Teller distortions, geometries for the complete series of Ru complexes were optimized using B3LYP/Lanl2DZ for comparison. Additionally, internal reorganization energies for oxidation were calculated to estimate hole conduction barriers, as described below.

Results and Discussion

We will first discuss the characterization of the oligomers via matrix-assisted laser desorption ionization−time-of-flight (MALDI-TOF) mass spectrometry and electrochemistry of both series **1** and series **2** tppz-bridged Ru oligomers, followed by discussion of the related ground-state electronic structures predicted by computational modeling. The qualitative pictures given by electrochemical characterization and theoretical methods will be contrasted, and predictions will be made for longer-length oligomers on the basis of both experiment and theory. Next, we discuss the experimental spectroscopy of the complexes and optical spectra predicted by INDO/S excited-state calculations, again comparing the results of spectroscopy, the computed semiempirical results presented here, and recent results by other groups. Finally, we will conclude with a discussion of the results presented and consequences for charge-transfer in these compounds in single-molecule devices.

Characterization of Complexes. In addition to MALDI-TOF and electrochemical characterization, discussed below, purity of the synthesized compounds was assessed using ^{1}H NMR. Data for monomeric, dimeric, and trimer **1c** complexes were identical with those of the literature, and the complexes showed high purity.[43] Other long oligomers (**1d**, **2c**,**d**), however, did not exhibit a significant ^{1}H NMR signal even with a high number of scans, likely due to the presence of a small amount of paramagnetic impurity (e.g., partially oxidized species). Consequently, characterization of the complexes via mass spectrometry and electrochemical methods is required.

1. Mass Spectrometry. In addition to electrochemistry and UV/vis spectroscopy, the ruthenium oligomers were characterized using MALDI-TOF. The desorption and ionization of the

(46) Becke, A. D. *J. Chem. Phys.* **1993**, *98*, 5648.
(47) Lee, C.; Yang, W.; Parr, R. G. *Phys. Rev. B* **1988**, *37*, 785.
(48) Dunnning, T. H.; Hay, P. J. In *Modern Theoretical Chemistry*; Schaefer, H. F., Ed.; Plenum: New York, 1976; Vol. 3, p 1.
(49) Hay, P. J.; Wadt, W. R. *J. Chem. Phys.* **1985**, *82*, 270.
(50) Wadt, W. R.; Hay, P. J. *J. Chem. Phys.* **1985**, *82*, 284.
(51) Hay, P. J.; Wadt, W. R. *J. Chem. Phys.* **1985**, *82*, 299.
(52) Zhan, C. G.; Nichols, J. A.; Dixon, D. A. *J. Phys. Chem. A* **2003**, *107*, 4184.
(53) Rienstra-Kiracofe, J. C.; Tschumper, G. S.; Schaefer, H. F.; Nandi, S.; Ellison, G. B. *Chem. Rev.* **2002**, *102*, 231.
(54) Rienstra-Kiracofe, J. C.; Barden, C. J.; Brown, S. T.; Schaefer, H. F. *J. Phys. Chem. A* **2001**, *105*, 524.
(55) de Oliveira, G.; Martin, J. M. L.; de Proft, F.; Geerlings, P. *Phys. Rev. A* **1999**, *60*, 1034.
(56) Curtiss, L. A.; Redfern, P. C.; Raghavachari, K.; Pople, J. A. *J. Chem. Phys.* **1998**, *109*, 42.
(57) DeProft, F.; Geerlings, P. *J. Chem. Phys.* **1997**, *106*, 3270.
(58) Muscat, J.; Wander, A.; Harrison, N. M. *Chem. Phys. Lett.* **2001**, *342*, 397.
(59) Hutchison, G. R. Theoretical Studies of Optics and Charge Transport in Organic Conducting Oligomers and Polymers: Rational Design of Improved Transparent and Conducting Polymers. Ph.D. Dissertation, Northwestern University, Evanston, IL, 2004.
(60) Ridley, J.; Zerner, M. *Theor. Chim. Acta* **1973**, *32*, 111.
(61) Reimers, J. R.; Hush, N. S. *J. Phys. Chem.* **1991**, *95*, 9773.
(62) Zeng, J.; Hush, N. S.; Reimers, J. R. *J. Am. Chem. Soc.* **1996**, *118*, 2059.
(63) Reimers, J. R. CNDO/S Program.
(64) Cances, E.; Mennucci, B.; Tomasi, J. *J. Chem. Phys.* **1997**, *107*, 3032.
(65) Cossi, M.; Barone, V.; Mennucci, B.; Tomasi, J. *Chem. Phys. Lett.* **1998**, *286*, 253.
(66) Cossi, M.; Scalmani, G.; Rega, N.; Barone, V. *J. Chem. Phys.* **2002**, *117*, 43.
(67) Tomasi, J. *Theor. Chem. Acc.* **2004**, *112*, 184.

Table 1. Electrochemical and Spectroscopic Data for the tpy-Capped and tppz-Capped Ruthenium Complexes as PF_6^- Salts[a]

compd	no.	formal potential (V) vs Ag/AgCl	opt abs (nm) (ϵ (10^{-4} cm^{-1} M^{-1}))	MS (*m*/*z*)	$\Delta E_{echem}/\Delta E_{spect}$ (eV)
$[Ru(tppz)_2]^{2+}$	**1a**	+1.56, −0.84	254, 318 (18.9), 357, 478 (5.95)	878,[b] $[Ru(tppz)_2]^+$	2.40/2.58
$[Ru_2(tppz)_3]^{4+}$	**1b**	+1.14, −0.25	256 (3.1), 298 (4.1), 325, 354 (3.4), 550 (1.9)	1802,[b] $[Ru_2(tppz)_3(PF_6)_3]^+$	1.39/2.26
$[Ru_3(tppz)_4)]^{6+}$	**1c**	+1.05, −0.24	253, 294 (6.6), 360 (5.9), 574 (3.4)	1857, $[Ru_3(tppz)_4 - 5H]^+$	1.29/2.16
$[Ru_4(tppz)_5]^{8+}$	**1d**	+0.91, −0.19	245, 289 (7.9), 372 (7.9), 463, 615 (4.8)	2347, $[Ru_4(tppz)_5 - H]^+$	1.1/2.02
$[Ru_n(tppz_{n+1})]^{2n+}$		+0.86, −0.13	245, 291, 373, 395, 669	NA	0.99/1.86
$[(tpy)(tppz)Ru]^{2+}$	**3**	+1.54, −0.91	274 (1.0), 283 (1.1), 308 (1.0), 474 (0.3)	723,[b] $[Ru(tpy)(tppz)]^+$	2.45/2.62
$[(tpy)_2Ru]^{2+}$	**2a**	+1.33, −1.21	232, 243, 272 (4.24[b]), 308 (7.04[b]), 335, 481 (1.58[b])	NA	2.54/2.60
$[(tpy)_2Ru_2tppz]^{4+}$	**2b**	+1.45, −0.30	242, 274 (5.1), 300 (5.4) 332, 374 (3.3), 548 (2.2)	1055,[b] $[Ru_2(tpy)_2(tppz)]^+$	1.75/2.27
$[(tpy)_2Ru_3(tppz)_2]^{6+}$	**2c**	+1.28, −0.28	263 (8.6), 316 (6.1), 374 (4.0), 560 (3.2)	1836, $[Ru_3(tpy)_2(tppz)_2(PF_6)_2 - 3H]^+$	1.56/2.22
$[(tpy)_2Ru_4(tppz)_3]^{8+}$	**2d**	+1.07, −0.20	236, 280 (8.1), 315 (7.8) 372 (6.9), 620 (5.5)	2010, $[Ru_4(tpy)_2(tppz)_3 - 7H]^+$	1.27/2.02

[a] Potentials for the trimer and tetramer (tpy and tppz) were measured using differential pulse voltammetry. [b] Reference 39.

oligomers in the MALDI process depends on the selection of the matrix, and the best results were obtained using the matrices α-cyano-4-hydroxycinnamic acid (CHCA) or 6-aza-2-thiothymine (ATT). Common features in all the spectra were the strong signals at 877 and 1511 Da originating from the monomer $[M - H]^+$ and dimer $[D + PF_6 - 2H]^+$, respectively. Using the ruthenium−tppz tetramer **1d** as an example, the most important characteristics, in general, for the oligomers in the MALDI spectra are the isotopic distribution patterns for each cluster of peaks and the mass of the highest peak in each cluster. The former illustrates that the peaks in the spectrum derive from species containing one or more ruthenium ions, and the latter allows identification of those species, on the basis of the mass of the most abundant ruthenium isotope (102 Da), since species seen in MALDI mass spectrometry are nearly always singly charged ions.[68] It is uncertain from the MALDI results alone whether the smaller oligomers were present in the original sample or resulted from in-source decay in the mass spectrometer. In general, MALDI is a soft ionization technique, but decomposition induced by the 337 nm laser pulses cannot be completely ruled out. In all cases, the mass spectral data were consistent with proposed stoichiometries. Decomposition of the tetramer to smaller oligomers might be expected, and all the abundant species related to the ruthenium tetramer **1d** were identified. (For more details, see Table S1.)

2. Electrochemistry. The first oxidation and reduction potentials for compounds **1a**−**d**, **2a**−**d**, and **3** are compiled in Table 1.

The monomers **1a**, **2a**, and **3** show one reversible, metal-localized oxidation corresponding to the II/III redox transition. At negative potentials, the reductions can be assigned as ligand-localized redox processes. A reversible one-electron oxidation peak is observed at +1.56, +1.33, and +1.54 V for Ru II/III oxidation states in complexes **1a**, **2a**, and **3**, respectively, and sequential one-electron reversible waves are observed at −0.84/−1.1 V (**1a**), −1.21/−1.42 V (**2a**), and −0.91/−1.36 (**3**), vs Ag/AgCl due to ligand reduction.[39] The **1a**, **2a**, and **3** variations in the formal potential for oxidation were influenced by the difference in π^* acidity of the ligands (tppz/tpy). Moreover, the dissimilarities in π^* acidity suggest stronger interactions among the metal and the tppz ligands implying a more stable ligand-localized reduction state.[69,70]

As discussed above, for dimers, a single two-electron oxidation wave would be anticipated in the limit of no interaction between the metal centers, and two one-electron oxidation waves are expected when communication exists across the bridging ligand. The difference in potential of these two waves depends on two effects: the interactions between metals and the change in electronic structure of the bridging ligand due to two bound metal centers. The oxidation potentials and the difference in potential between them are +1.7/+1.45 V, 250 mV vs Ag/AgCl, for complex **2b** and +1.60/+1.14 V, 460 mV vs Ag/AgCl, for complex **1b**. Thus, there is greater communication for the tppz-capped dimer **1b** (i.e., $\Delta E^{\circ\prime}$ value of 250 and 460 mV for **2b** and **1b**, respectively), consistent with the greater π^* acidity of the tppz ligand. (For more details, see Table S2.) Scanning in the negative direction a one-electron wave is observed, assigned to the bridging tppz at −0.25 (**1b**), at lower potential than expected, compared to the monomers. The bonding of a second metal has stabilized the π^* orbital of the bridging tppz. Interaction with the metal centers and stabilization of the π^* levels result in another one-electron reduction wave from the bridging ligand. In other words, the bridging ligand can be reduced twice before the reduction of a singly bound tppz ligand is observed. This second reduction shows at −0.80 V, before the observation of the $2e^-$ single wave of the capping-tppz ligands (the same is observed for **2b**).[39]

The voltammetric response of the trimetallic species containing tpy or tppz as capping groups, **1c** and **2c**, is shown in Figures 3 and S9. At positive potentials, **1c** and **2c** exhibit three one-electron oxidations waves at +1.83, +1.51, +1.05 V and 1.73, +1.49, +1.28 V, respectively (Figures 3 and S9**).** We assign these three waves to the Ru(II/III) oxidation, one electron for each metal center. As mentioned above, the bridging tppz ligands are expected to have reductions at low potentials, and since the trimetallic species have two bridging tppz ligands, one would anticipate two sets of closely spaced reductions as we, in fact, observed at −0.24, −0.40, −0.81, −1.05 (for **1c**) and −0.28, −0.42, −0.74, and −0.99 (for **2c**); these two sets of low lying reductions are clearly indicative of the presence of two bridging tppz ligands. If the potential is scanned past −1.65 V (Figure 3), the reduction of the terminal tppz ligands is observed as a single 2-electron wave (**1c**). The difference of more than 1 V in the reduction potential between the tppz ligands bound to one metal and tppz bound to two metals demonstrates a significant change in the electronic structure of the tppz bridging ligand.

In the trimetallic (**1c** and **2c**) and tetrametallic (**1d** and **2d**) complexes, as seen in Table 1 and illustrated in Figures 3, S7, and S9, the first oxidation potentials decrease but the first reduction potentials increase (becoming less negative), suggesting continuing delocalization and electronic communication and

(68) Karas, M.; Gluckmann, M.; Schafer, J. *J. Mass Spectrom.* **2000**, *35*, 1.
(69) Sutton, J. E.; Taube, H. *Inorg. Chem.* **1981**, *20*, 3126.
(70) Sutton, J. E.; Sutton, P. M.; Taube, H. *Inorg. Chem.* **1979**, *18*, 1017.

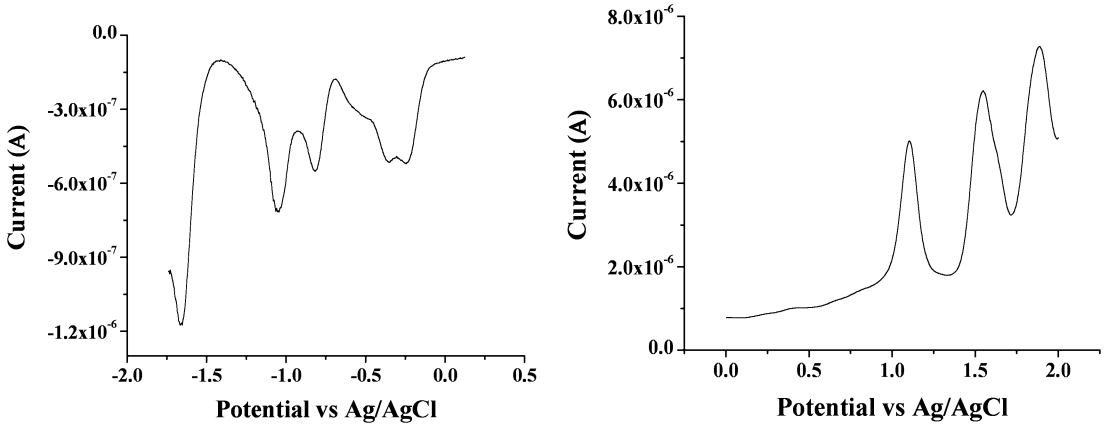

Figure 3. Differential pulse voltammetry of **1c** using a glassy carbon disk electrode in 0.1 M tetra-*n*-butylammonium hexafluorophosphate/acetonitrile. Amplitude = 50 mV, pulse with = 50 mV, and pulse period = 200 ms.

Table 2. Computed Gas-Phase HOMO, LUMO, and Band Gap Energies (in eV) for Compounds Studied (Series **1a**−**f**, **2a**−**f**) Using both INDO and DFT (B3LYP/Lanl2DZ) Calculations, as Well as INDO/S Excitation Energies

		INDO				DFT		
compd	no. of Ru atoms	HOMO	LUMO	gap	excitation	HOMO	LUMO	gap
1a	1	−12.472	−6.192	6.280	3.26	−10.759	−7.638	3.122
1b	2	−15.407	−10.560	4.846	2.72	−13.288	−11.958	1.331
1c	3	−17.331	−13.439	3.892	2.53	−15.102	−14.457	0.645
1d	4	−18.766	−16.015	2.751	1.76	−16.709	−16.579	0.130
1e	5	−19.899	−17.983	1.915	1.07			
1f	6	−20.845	−19.809	1.036	0.32			
2a	1	−12.898	−6.280	6.617	3.13	−11.076	−7.718	3.358
2b	2	−16.474	−10.766	5.709	2.55	−14.597	−12.136	2.462
2c	3	−18.878	−13.634	5.244	2.99	−16.940	−14.720	2.220
2d	4	−20.587	−16.173	4.415	2.94	−18.584	−17.107	1.477
2e	5	−22.061	−18.218	3.843	2.56	−20.100	−19.261	0.839
2f	6	−22.967	−19.925	3.042	1.69			

a decrease in the energy gap of the complexes. The diminution of the energy gap takes place due to an increase in stability of the LUMO state and the decrease in stability of the HOMO state. The destabilization in the HOMO level is, in part, associated with repulsion of charges between metal centers in the molecules as previously suggested by Taube[69,70] accompanied by changes in the π^* orbital of the ligand (LUMO). In addition, this modulation of the π^* orbital reflects a stabilization of the LUMO level suggesting a strong interaction among the π^* orbitals of the ligands and the d(π) symmetry nonbonding orbitals of the metals (i.e., π-back-bonding). In short, π-back-bonding is responsible for the decrease in the band gap of the molecules. This ΔE_{gap} trend appears to be linearly correlated with the reciprocal of the number of metal centers—a "1/*N*" relationship similar to that observed in organic conjugated oligomers and polymers—and is approximate only for short oligomer lengths.[71−74]

Incomplete reactions or the presence of impurities can be easily identified by new waves between +0.8 and −0.1 V vs Ag/AgCl. For example, reactions with oxygen leading to Ru−oxo complexes, or inner-sphere chloride salts, are electrochemically active in the same range. These oxo and chloro complexes can be easy identified using electrochemistry. Figure S8 illustrates an impure trimer, **1c**. Thus, the purity of the complexes can be easily verified by the presence of waves in the range mentioned above and also as differences in the background current between the peaks. The high quality of the CV and DPV obtained demonstrates the absence of electrochemically active impurities in all oligomers studied here.

Computed Electronic Structure. Since synthesis and especially purification of transition-metal oligomers can be quite time-consuming, the possibility of predicting the electronic structure and optical properties of these complexes by first-principles or semiempirical calculations is an attractive prospect. Since the computational complexity and resources required for calculations on larger transition-metal species are very large (e.g., calculations with B3LYP/Lanl2DZ single-point energies on compound **1d** involving 234 atoms can require several days), it is also important to balance such promise against the accuracy of the methods.

Table 2 compiles the predicted HOMO and LUMO levels from INDO and B3LYP/Lanl2DZ methods (illustrated in Figures S1 and S2) for compounds **1a**−**f** and **2a**−**f**, as well as the predicted HOMO−LUMO energy gap and the INDO/S excitation energies. As illustrated in Figure 4 for series **1** compounds $[Ru_n(tppz)_{n+1}]^{2n+}$, the electronic structure quickly develops a high density of states in both the occupied and unoccupied orbitals, and the DFT-predicted energy gap decreases dramatically to almost zero for $[Ru_4(tppz)_5]^{8+}$, as indicated in Figure 5. Importantly, unlike the trend in oxidation and reduction potentials measured by electrochemistry mentioned above, the computed ionization potentials from both

(71) Hutchison, G. R.; Zhao, Y. J.; Delley, B.; Freeman, A. J.; Ratner, M. A.; Marks, T. J. *Phys. Rev. B* **2003**, *68*, 035204.
(72) de Melo, J. S.; Silva, L. M.; Arnaut, L. G.; Becker, R. S. *J. Chem. Phys.* **1999**, *111*, 5427.
(73) Taubmann, G. *J. Chem. Educ.* **1992**, *69*, 96.
(74) Kuhn, H. *J. Chem. Phys.* **1949**, *17*, 1198.

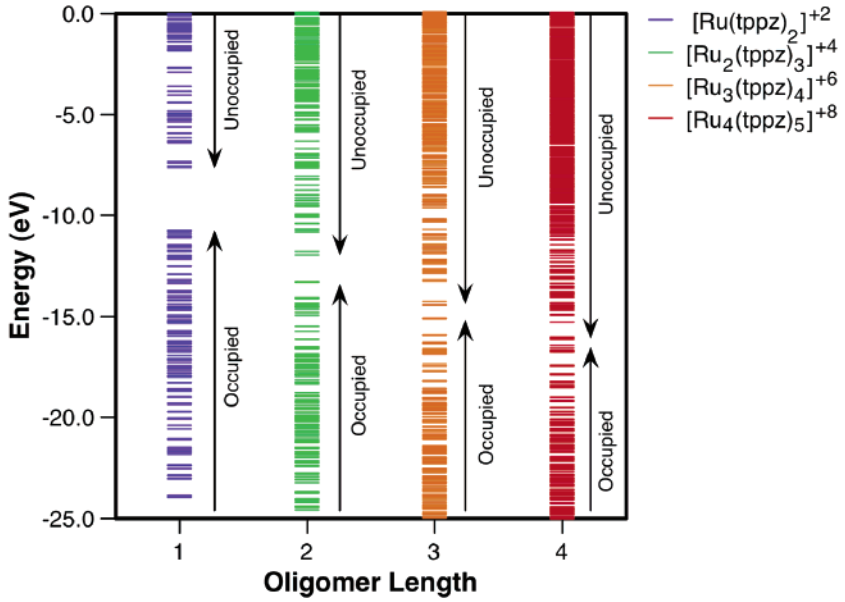

Figure 4. Orbital energies for series **1** compounds $[Ru_n(tppz)_{n+1}]^{2n+}$ computed by B3LYP/Lanl2DZ in the gas phase, indicating both occupied and unoccupied orbital ranges. Note that the computed ionization potentials, as represented by the HOMO energy, increase as a function of oligomer length as does the electron affinity, as represented by the LUMO energy. The same trend is observed for the orbital energies obtained for the INDO method, as these gas-phase methods account for the increasing overall cationic charge for longer oligomers.

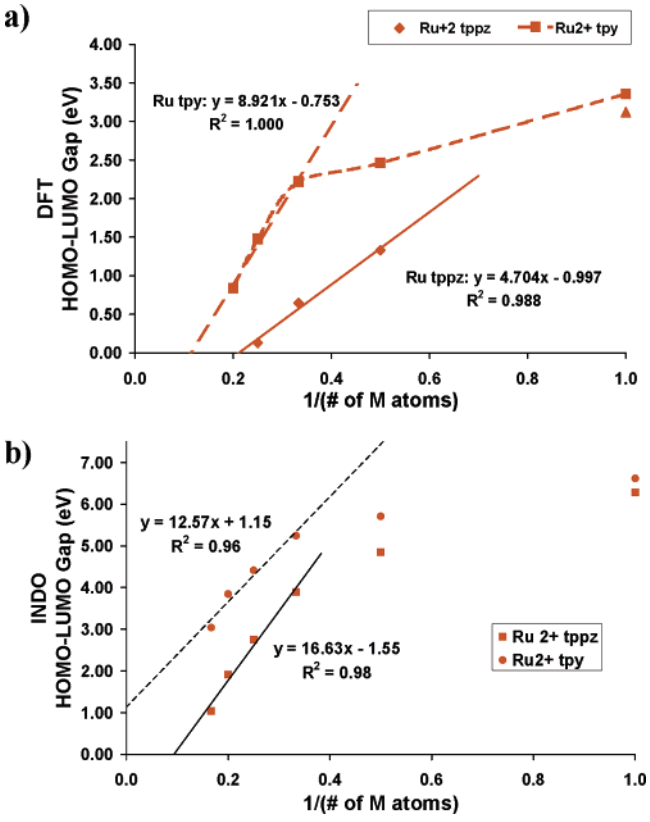

Figure 5. Trends in the computed ground-state HOMO−LUMO gaps for $[Ru_n(tppz)_{n+1}]^{2n+}$ and $[(tpy)_2Ru_n(tppz)_{n-1}]^{2n}$, as a function of 1/(no. of metal atoms) using (a) DFT (B3LYP/Lanl2DZ) and (b) INDO. Note that both DFT and INDO methods indicate trends for two regimes for all compounds—a relatively shallow slope at small chain lengths (i.e., $n \leq 3$) with different HOMO−LUMO gaps for each transition metal and a steep slope for longer chain lengths ($n \geq 3$) with HOMO−LUMO gaps essentially independent of metal ion. Both methods also predict zero HOMO−LUMO gap for finite-length tppz-capped oligomers for all metals.

INDO and B3LYP methods increase dramatically, as do the electron affinities. As these calculations do not take dielectric screening into account, this trend is not surprising, although recent DFT calculations utilizing a PCM solvation model to account for the solvent dielectric also showed an increasing trend in ionization potentials for compounds **1a**−**d**,[43] which suggests that such models do not properly account for the highly charged nature of these species. Similar PCM results discussed below exhibit the same trend. In short, while isolated mononuclear complexes with low ionic charge may be described appropriately by gas-phase or PCM theoretical models, the electronic structures of multimetallic complexes with high ionic charge are not well-described, regardless of dielectric screening models.

As illustrated in Figure 5, the gas-phase electronic structure of transition-metal tppz compounds as a function of $1/N$ shows two linear regimes as computed by B3LYP/Lanl2DZ and INDO. The first regime from ∼1−3 metal centers shows a small slope against $1/N$, while the second regime for oligomers with three or more metal centers exhibits a high slope indicative of high delocalization. Since recent literature has demonstrated problems with predicting the electronic structure of highly delocalized conjugated species with DFT,[75,76] the INDO method was used to confirm the qualitative picture of the trends in electronic structure. While DFT predicts that the tppz-capped series **1** oligomers should have zero band gap at ∼5 metal centers, the trend predicted by the INDO method still suggests convergence to zero band gap, though at ∼10 metal centers. If this picture is accurate, then band-type conduction might be observed in single-molecule or gas-phase measurements of long-length tppz-capped oligomers. However, the gas-phase calculations, particularly those with low HOMO−LUMO gaps, have poor correlation with the experimental electrochemical redox gaps presented here (i.e., in Figures 3, 5, and 7 and Tables 1 and 2), which show only one linear regime, likely because the gas phase calculations do not consider dielectric screening in solution and counterions. Consequently, these computed energies and

(75) Cai, Z. L.; Sendt, K.; Reimers, J. R. *J. Chem. Phys.* **2002**, *117*, 5543.
(76) Reimers, J. R.; Cai, Z. L.; Bilic, A.; Hush, N. S. In *Molecular Electronics III*; New York Acad. Sciences: New York, 2003; Vol. 1006, p 235.

HOMO−LUMO gaps exhibit a high "charging penalty," particularly for the 6+, 8+, and 10+ trimers, tetramers, and pentamers, respectively. The use of solvent models to partially correct for this effect is discussed below. However, both the computed electronic structure, and the computed orbital contours (Table S3), particularly for the LUMOs clearly illustrated the high degree of communication between all metal centers in the complexes and the delocalization along the entire oligomer.

Interestingly, though the effect of end caps would naively be expected to diminish for long oligomers, the difference between tpy-capped series **2** and tppz-capped series **1** is predicted by both DFT and INDO to remain large *regardless* of the oligomer length. Quite surprisingly, the bis-tpy and bis-tppz monometallic species have almost identical energy gaps, while computed energy gaps for series **2** and series **1** often differ by >0.5 eV. This effect is consistent with the electrochemical characterization of series **1** and **2**, which exhibit a constant 0.28 eV difference in ΔE_{redox} across $n = 1-4$ oligomers synthesized here. Thus, the degree of electronic communication across each oligomer is high enough that the effect of end-group substitution shows up even for oligomer **2d**, $[(tpy)_2Ru_4(tppz)_3]^{8+}$, which is 34.5 Å in length.

As mentioned above, the geometries used for the computational study are predicted via the UFF molecular mechanics force field. Since molecular mechanics methods do not consider the electronic structure, these geometries do not account for potential Peierls distortions of the pseudo-one-dimensional chain compounds. Indeed, for all compounds considered, there is a constant 6.79 Å Ru−Ru separation across the bridging TPPZ ligands. Consequently, geometry optimizations of series **2** tpy-capped monomer, dimer, trimer, and tetramer were performed to consider the quality of the molecular mechanics geometries (particularly the degree of Peierls distortion) and any consequences on the computed electronic structure.

In all cases, the effect of the Peierls distortion is very small (e.g., 0.016 Å difference in Ru−Ru distance for compound **2d**) because the TPPZ framework is very rigid. Consequently, for rigid ligands such as TPPZ, the UFF molecular mechanics method appears to be an excellent, computationally efficient model for the ground-state geometries of transition-metal oligomers.

As mentioned above, the solvent dielectric PCM model was used in an attempt to correct for the discrepancies between the gas-phase calculations and the solution-phase electrochemistry and spectroscopy presented here. Unfortunately, both the current results (illustrated in Figure S3) and previous results[43] (Figure S4) demonstrate that the PCM models do not properly correct the computed ground-state electronic structure. For example, both the gas-phase calculations above and the solution-phase electrochemistry illustrate that the tpy-capped series **2** oligomers have a larger HOMO−LUMO gap than the tppz-capped series **1** oligomers. On the contrary, Figure S3 illustrates that the PCM-computed HOMO−LUMO gaps of series **2** are comparable or *smaller* than the analogous series **1** oligomers. Furthermore, while Figure 6 illustrates that, for an infinite-length polymer of series **1**, the electrochemical band gap would be ~0.5 eV, the trends from computed HOMO−LUMO gaps in Figure S3 (albeit only from monomers and dimers) suggest a limit of ~2.17 eV for series **1** and ~1.72 eV for series **2** infinite polymers. Similar PCM computational results[43] on series **1** compounds similarly

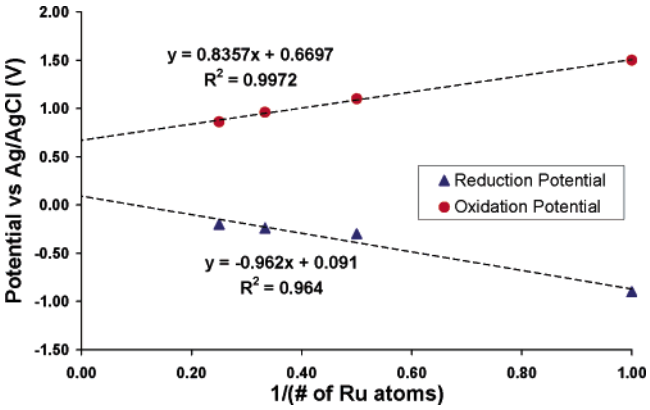

Figure 6. Trends in oxidation and reduction potentials of series **1** compounds $[Ru_n(tppz)_{n+1}]^{2n+}$ as a function of 1/(no. of Ru atoms). Note that, for an infinite-length polymer, the trends indicate ~0.5 eV band gap, though the increasingly positive reduction potential would suggest the $+2n$ oxidation state would not be electrochemically stable. The reduction potential crosses 0.0 V vs Ag/AgCl at ~10.5 Ru atoms.

suggest a HOMO−LUMO gap of ~1.34 eV for the infinite polymer (Figure S4). In all cases, while the PCM computational results show a finite HOMO−LUMO gap for all oligomer lengths, unlike the gas-phase calculations noted above, the results are substantially too large when compared with experimental electrochemical data. Finally, as noted above, the computed ionization potentials from PCM results presented here and in previous work[43] incorrectly increase as a function of oligomer length, much like the gas-phase calculations.

Spectroscopy. The UV/vis spectra for monomer and dimer molecules of both series **1** and series **2** and **3** have been well studied.[25,29,32−39,43] Moreover, it has been shown that these transitions are primarily ligand-localized transitions and metal to ligand charge transfer (MLCT) transitions—with the ligand-localized transition bands observed in the UV region and MLCT transitions observed in the visible region of the spectrum. Thus, the lowest excited state is typically assigned as an MLCT d−π* transition. For the dimers **1b** and **2b**, the $\pi-\pi$* ligand transitions shift to lower energy due to the stabilization of the π* orbital on the bridging ligand derived from bonding to a second metal. The ligand-localized transitions in bimetallic compound **1b** are found at 298, 325, and 354 nm. The dimer also exhibits a MLCT at 550 nm, well-known to be a d−π* excited state.[39] The spectroscopic energy gap observed for the dimer **1b** is 0.32 eV smaller than that of the monomer **1a** (similar results are found for **2a**,**b**). This large difference in excitation energy between monomers and dimers is related to the Ru_1-Ru_2 communication, resulting in stabilization of the LUMO orbital and delocalization of the electron in the dimer molecule.

The UV/vis spectroscopy of the longer trimer, tetramer, and polymer compounds exhibit expected trends with the stabilization of the ligand π*-orbitals, yielding lower energy peaks for these species than in the monomer and dimer. The UV spectra of polymer showed peaks at 245, 291, 373, 395, and 673 nm. The optical transitions in the polymer, tetramer, or trimer species are more difficult to assign exactly. However, it is well-known that, for these complexes, the lowest excited state is a MLCT transition, and these were observed at 478, 550, 574, and 615 nm, for tppz-capped complexes **1a**−**d** and 474, 481, 548, 560, and 620 nm for tpy-capped complexes **3** and **2a**−**d** (spectral data are collected in Table 1). Figure 7 illustrates that while

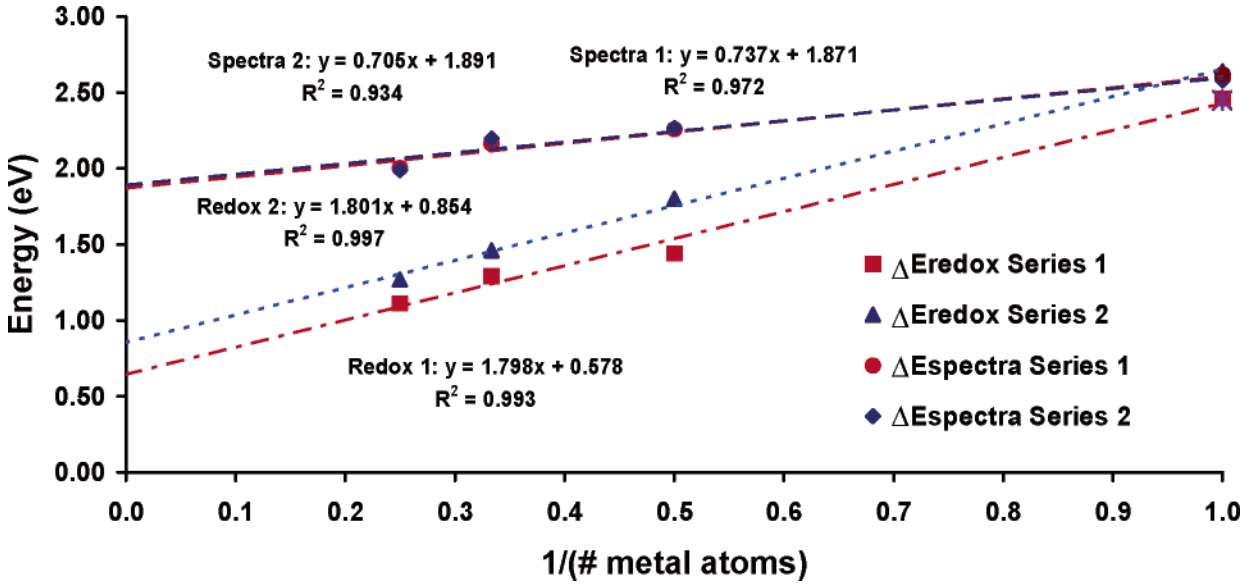

Figure 7. Trends in optical excitation energies ($\Delta E_{spectra}$) for series **1** compounds $[Ru_n(tppz)_{n+1}]^{2n+}$, represented by the lowest energy transition, compared to the difference in electrochemical reduction and oxidation peaks (ΔE_{redox}) for series **1** and series **2** and **3** compounds. Note that the optical excitation energies are consistently higher in energy than the electrochemical measurements and that the tpy-capped series **2** compounds show a consistently higher electrochemical ΔE_{redox} than the tppz-capped series **1** compounds.

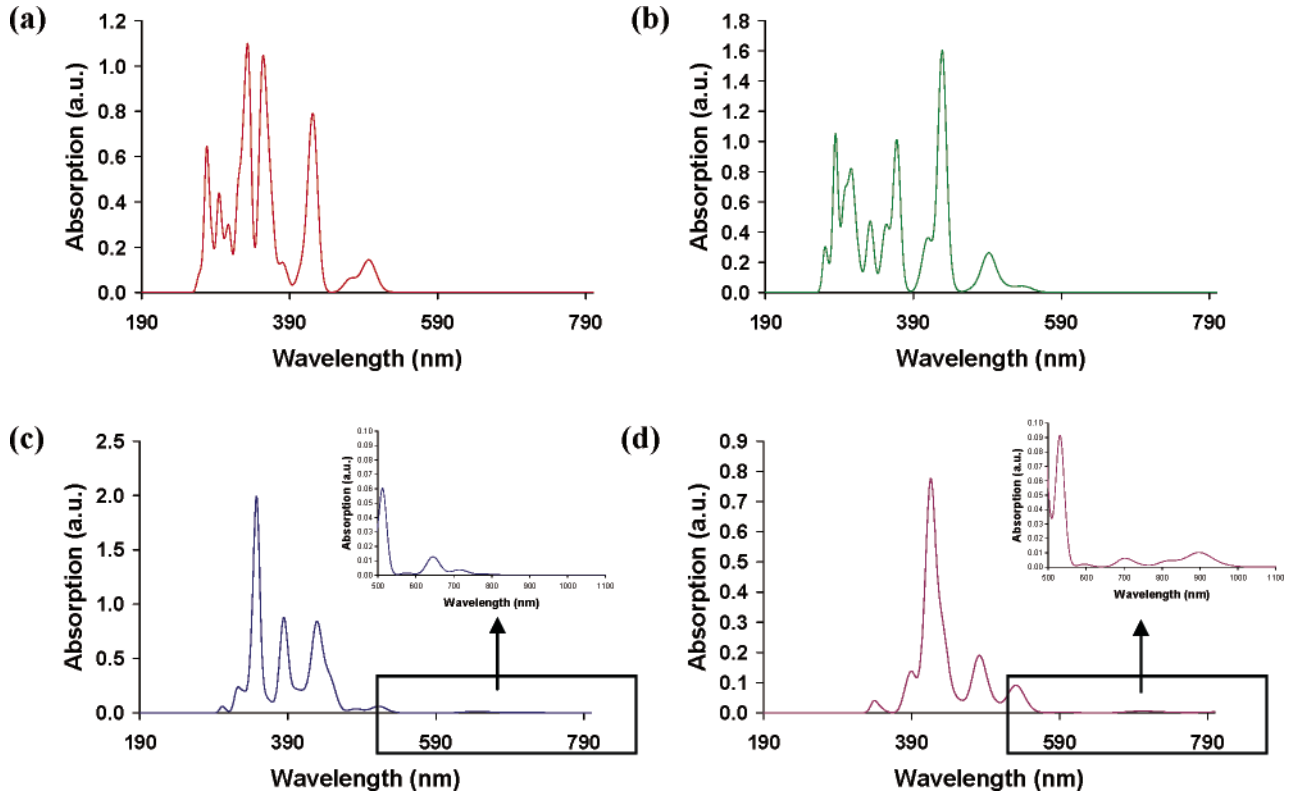

Figure 8. Computed INDO/S optical excitation spectra for (a) $[Ru_2(tppz)_3]^{4+}$, (b) $[Ru_3(tppz)_4]^{6+}$, (c) $[Ru_4(tppz)_5]^{8+}$, and (d) $[Ru_5(tppz)_6]^{10+}$ using the 400 lowest energy optical excitations and Gaussian broadening applied. Note that, for the tetramer and pentamer, low-energy transitions are predicted with very low oscillator strength.

this trend also shows ~1/*N* correlation with the number of metal centers, the observed optical transitions are at significantly higher energy than observed from electrochemistry. This implies that either the frontier orbitals have symmetry-forbidden transitions or the existence of lower-energy transitions, which would be in the near-infrared region for the trimer and tetramer complexes, which have not been examined by previous studies utilizing only UV/vis spectra.[39,43]

The present UV/vis/NIR spectroscopy data indicate weak absorptions at lower energies overlapping with the MLCT peaks for longer oligomers (series **1** and **2** molecules **c** and **d**). This low-energy tail can be attributed to spin-forbidden transitions.[43] For the monomer, phosphorescent states are well-known as $MLCT^3$ transitions,[77,78] and these radiative pathways are ascribed to four $MLCT^3$ levels (over a range of 400 cm^{-1} difference). Analogous to the singlet states, the triplet states are also affected

by the second metal coordination to additional metal atoms, and thus, such long-wavelength tails are observed in the longer oligomers.

Computed Optical Excitations. Computational methods for predicting optical excitation spectra can distinguish between low-intensity forbidden transitions and significant transitions outside the UV/vis window, since all possible low-energy transitions would be computed. Recent work used time-dependent density functional theory (TDDFT) with a dielectric solvent model and demonstrated high correlation with experimental tppz-capped series **1a**−**c** optical spectra.[43]

On the other hand, for many organic π-conjugated oligomers and polymers and transition metal complexes, the semiempirical INDO/S methodology has proved to be highly accurate and computationally efficient and does not explicitly include a dielectric solvent model. Examples of computed optical excitation spectra for series **1** are shown in Figure 8. Despite the lack of a dielectric solvent model, the optical excitation spectra computed via the INDO/S method show a high degree of correlation with the experimental optical UV/vis/NIR spectra shown in Figure 9. Importantly, despite the fact that the ground-state INDO electronic structure shows a trend toward zero HOMO/LUMO gap for series **1** (Figure 5b), the predicted optical excitations show slightly higher energy MLCT transitions than observed in the experimental spectra. Indeed, there appears to be a "compression" of the various optical excitations predicted via INDO/S, such that the experimentally observed ligand transitions at 200−400 nm are predicted to occur at slightly longer wavelengths, and the MCLT transitions observed experimentally at 500−800 nm are predicted to occur at ∼400 nm. However, the INDO method does accurately indicate a weak tail from spin-forbidden transitions at long wavelengths (Figure 8c,d).

The mis-scaling of the optical excitations predicted by INDO likely indicates a deficiency in the INDO/S parameters for Ru—not surprising since the parameters were derived from monometallic $[Ru(bpy)_3]^{+2}$ studies.[61,62] However, the high correlation between computed and experimental optical spectra suggests that the solvent dielectric model may not be the largest source of error in the ground-state electronic structure computed by DFT and INDO as discussed above. Instead, the lack of explicit counterions to balance the high positive charge is probably a more important factor than the dielectric environment. Nevertheless, these results help elucidate the excited state and charge transport properties of the oligomers.

Consequences for Charge-Transfer and Transport Properties. Important questions have emerged about the electronic structure and properties of band formation in these highly charged transition metal oligomers, as described above. For molecular electronics applications, understanding the nature of the charge-transfer process is essential. The electrochemical characterization and predicted ground-state electronic structure suggest a high degree of delocalization in these species and thus significant electronic coupling between metal centers. Additionally, the frontier orbitals (e.g., HOMO and LUMO contours in Table S3) exhibit coupling of multiple metal centers and delocalization over multiple ligands, again suggestive of a high

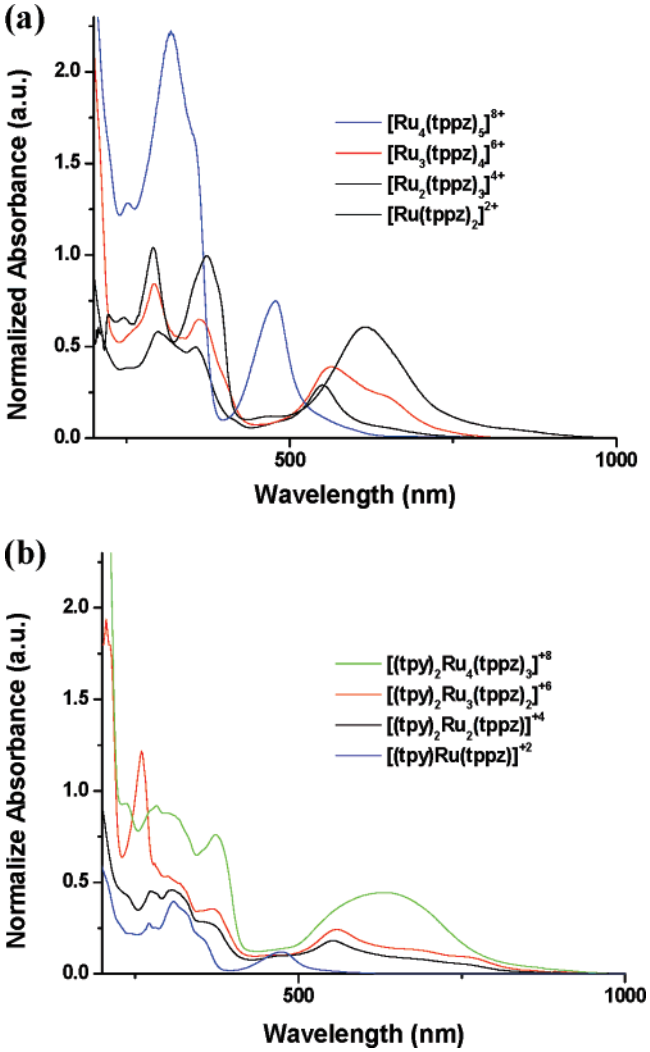

Figure 9. Experimental UV/vis/NIR optical absorption spectra for (a) series **1** and (b) series **2b**−**d** and **3** compounds. Note that, for all compounds, a long, weak absorption tail extends to ∼1000 nm, particularly for the longer oligomers. Data were normalized to a concentration of 1.1×10^{-6} μM (series **1**) and 6.33×10^{-7} μM (series **2**).

degree of electronic coupling. Figure 4 is suggestive of the onset of bandlike electronic structure in long oligomers of series **1** and **2**, but more detailed analysis of the potential charge-transfer pathways is needed. In particular, consideration of the reorganization energies for small length oligomers (e.g., monomers and dimers) under oxidation or reduction should suggest the likely charge-transfer mechanism through these molecular wires.

The reorganization energy (λ) is defined as the barrier to hole or electron transport caused by geometric reorganization from the oxidation or reduction of a particular species. For the following discussion, we will focus on the internal reorganization energy of the molecule itself and neglect any environmental (outer-sphere) reorganization since in many molecular wire environments, no bulk solvent is present. If the reorganization energy λ, is much greater than the electronic coupling, then charge transport is typically assumed to occur via some sort of hopping mechanism rather than metallic band transport.[79−81] The

(77) Kalyanasundaram, K. *Photochemistry of Polypyridine and Porphyrin Complexes*; Academic Press: London, San Diego, 1992.
(78) Batista, E. R.; Martin, R. L. *J. Phys. Chem. A* **2005**, *109*, 3128.
(79) Barbara, P. F.; Meyer, T. J.; Ratner, M. A. *J. Phys. Chem.* **1996**, *100*, 13148.
(80) Berlin, Y. A.; Hutchison, G. R.; Rempala, P.; Ratner, M. A.; Michl, J. *J. Phys. Chem. A* **2003**, *107*, 3970.
(81) Johansson, E.; Larsson, S. *Synth. Met.* **2004**, *144*, 183.

Table 3. Computed Internal Reorganization Energies (λ) Using B3LYP/Lanl2DZ Geometries for First Oxidation and Reduction Processes of Each Compound

	internal reorganizatn energy (eV)	
complex	oxidn	redn
$[Ru(tpy)_2]^{+}$	0.064	0.128
$[(tpy)_2Ru_2(tppz)]^{4+}$	0.169	0.515

internal reorganization energies for hole and electron transfer were computed using the DFT-computed geometries of the original, oxidized, and reduced species, using previously reported methods.[80,82] The results are compiled in Table 3. The surprisingly small internal reorganization energies, particularly for oxidation, are not entirely unanticipated. For oxidation of a Ru(II) complex to Ru(III) complex, the hole is localized on the metal center, and only small changes in geometry occur—mostly very small changes in the Ru−N bond distances. Consequently, it is expected that these species should exhibit bandlike transport, particularly for hole transport. For reduction, the internal reorganization energies are larger, as the added electron localizes on the π-conjugated organic ligands, resulting in greater geometric changes than for oxidation. The computed internal reorganization energies for reduction are in line with those computed for *reduction* of isolated conjugated/aromatic organic molecules such as benzene or conducting polymers.[80,82] Further studies should consider the band structure of tppz-bridged Ru chains to estimate the electronic coupling between metal centers and provide estimates of charge-transport properties.

Conclusions

Two series of ruthenium oligomers with the tppz π-bridging ligand with lengths from 1 to 4 Ru atoms have been synthesized and fully characterized via electrochemistry, spectroscopy, MALDI-TOF mass spectrometry, and computational modeling. The use of both terpyridine and tppz-capped oligomers demonstrates the sensitivity of the complexes to ligand substitution. In particular, the end substitution results in a difference of 0.5 V between the ΔE_{redox} of the tpy-capped and tppz-capped species—an effect which is consistent over the entire series of oligomers. The full analysis of the electronic structure of these compounds demonstrates the high degree of electronic coupling and tremendous potential for highly conductive one-dimensional molecular wires in transition-metal oligomers. The low reorganization energies suggest that these species should exhibit metallic bandlike charge transfer of both holes and electrons, but further studies of the band structure of these materials are needed for a full understanding of the transition from quantized molecular electronic states to a bandlike continuum electronic structure. Future computational modeling of large (and thus highly charged) metal oligomers should focus on the inclusion of explicit counterions rather than dielectric solvation models.

Acknowledgment. We thank the NSF/NIRT program (Grant CHE-0403806) for support. This work was also supported in part by a computer resource grant from the University of Minnesota Supercomputing Institute and from the Cornell Center for Materials Research computing facility.

Note Added after ASAP Publication. After this paper was published ASAP on January 17, 2006, changes were made in Table 1, column 5, rows 2, 3, and 6. The corrected version was published ASAP January 23, 2006.

Supporting Information Available: A complete citation list for ref 45, tables of full mass spectrometry and electrochemical data, figures of trends in computed HOMO and LUMO levels for DFT and INDO methods, figures illustrating the comparison of gas-phase and PCM solvation model DFT calculations, the geometry of compound **1e**, and an example of a MALDI spectrum, figures of the differential pulse voltammetry of a pure and impure sample of compound **2c** and the cyclic voltammetry of compound **1d** with elaborated discussion of the electrochemistry for compound **2c** and **1d**, trends in the oxidation potential for series **1**, **2b**−**d**, and **3**, computed HOMO and LUMO isosurfaces for series **1**−**3**, and a figure of overlapping experimental UV/vis spectra and computed INDO/S optical excitations. This material is available free of charge via the Internet at http://pubs.acs.org.

JA0552139

(82) Hutchison, G. R.; Ratner, M. A.; Marks, T. J. *J. Am. Chem. Soc.* **2005**, *127*, 2339.